Application of Hardware-in-the-Loop environment in the simulation of thermal systems

Predrag Nikolić, Pavle Stepanić
Computer Controlled Systems
Lola Institute Ltd
Belgrade, Serbia
predrag.nikolic@li.rs, pavle.stepanic@li.rs

Velimir Čongradac
Department of Automatic Control
Faculty of Technical Sciences
Novi Sad, Serbia
velimir@uns.ac.rs

***Abstract*— With the rising energy costs, there is an increasing interest in energy efficiency in building construction supported by computational tools. This paper describes the design and implementation of a Hardware-In-the-Loop (HIL) system for the development of a thermal zone simulation and control system. The practical part of the work covers the implementation of the HIL approach using appropriate hardware and software environments. A dynamic model of a thermal zone is developed, which integrates a heating system (radiator) with the ability to control the mass flow of hot water inflow to it.**

Keywords—HIL, thermal zone, building systems, PID

I. Introduction

The increasing demand for energy resources, driven by rising living standards, has influenced energy prices globally [1]. This has heightened interest in the field of energy efficiency and the tools that support its development [2]. To address these challenges, engineers have relied on computational tools to develop solutions aimed at improving energy efficiency in building systems. A critical concept in building systems is a thermal zone, which represents a division of a building into distinct thermal zones, allowing for climate control that meets the specific comfort needs of occupants - effectively reducing the heating or cooling energy demand in occupied spaces [3]. One potential solution considered in this study is the simulation of a thermal zone in a Hardware-in-the-Loop (HIL) system as a tool for enhancing energy efficiency in building systems. Although HIL systems are often used in automotive, aerospace, military, and energy industries [4,5]. Promising results have also been achieved in residential and commercial building systems [6].

The application of HIL in building energy systems allows for the testing of integrated energy systems, which combine heating, cooling, and power supply functionalities [7]. Such integration is essential for achieving optimal performance in smart buildings, where energy efficiency is paramount [8]. The idea is to model mathematically, implement it on a hardware platform, and test the simulation of a thermal zone. With a sufficiently accurate mathematical model, many scenarios could be tested, one of which is observing a disturbance when two individuals enter the zone and engage in sitting and light work activities. This could potentially enable the selection of optimal parameters that might contribute to energy efficiency.

This research has been supported by the research grants of the Serbian Ministry of Science, Technological Development and Innovations, grant No. 451-03-66/2024-03/ 200066..

The process model requires a detailed description of the set of differential equations governing the system dynamics, including energy flows, mass flows, and parameter changes. This paper is divided into five sections. In Section II, the architecture of the HIL system is described, as well as the definition of the thermal zone. Furthermore, the derived mathematical model of the thermal zone is presented in Section III. Experimental testing utilizing appropriate software and hardware tools is presented in Section IV. In section V, the obtained results will be analyzed, providing further insights into the model's performance and offering guidelines for improving both the model and the entire HIL system for simulating thermal processes. Conclusions are given in Section VI.

II. Preliminaries

A. Arhictecture of HIL system

HIL simulation is a powerful technique widely used in engineering fields to test and evaluate the performance of complex dynamic systems [9]. It acts as a bridge between virtual simulations and real-world system processes.

Some of the reasons for using HIL systems include:

- Facilitated manipulation of zone elements compared to real-world processes.
- Increased time efficiency, enabling continuous testing and placing the system under desired conditions.
- Reduced travel and operational costs, as engineers do not need to be physically present at the process location.

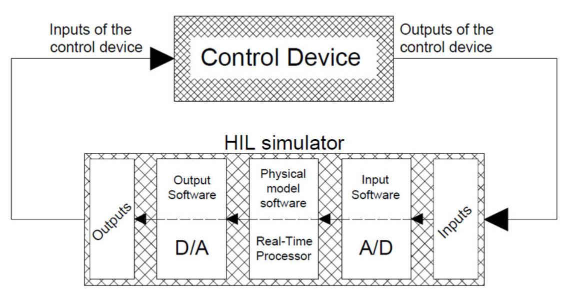

Fig. 1. HIL configuration

HIL represents a configuration in which a control device is integrated into a loop with the hardware simulating the process. The control device interacts with the simulated system in real-time, receiving inputs and sending outputs as it would in a real-world application. This setup allows engineers to test control algorithms and system responses under controlled and repeatable conditions without the need for a fully operational physical system.

B. *Thermal zone*

A thermal zone represents a room or a group of rooms within a building that share similar requirements for maintaining the following parameters: air temperature, relative humidity, CO_2 concentration, and lighting.

Rooms that form a single thermal zone may or may not be physically separated. A building can have multiple thermal zones, each equipped with an independent heating and cooling source.

Due to differences in purpose, occupancy, and solar radiation, each zone requires specific parameter settings to ensure optimal conditions. As a result, zoning or managing the parameters of individual zones emerges as an appropriate solution. It is worth noting that zoning can lead to significant energy savings compared to, for instance, heating the entire building, as it focuses on actively used zones [10].

III. Mathematical model of the thermal zone

A. *Initial balance equation*

The model will be based on the thermal energy balance equation of heat gains and losses within the zone. It is defined as:

$$\dot{Q}_z+\dot{Q}_i=\dot{Q}_p+\dot{Q}_w \tag{1}$$

Here, $\dot{Q}_z$ represents the heat losses through the zone's thermal envelope, $\dot{Q}_i$ denotes the heat losses due to infiltration through door and window gaps, $\dot{Q}_p$ indicates the gain from occupants, and $\dot{Q}_w$ represents the heat gain from the heating unit.

B. *Model of the thermal envelope*

The calculation of the zone's heat losses is based on the EN 12831 standard [11]. It is divided into transmission and ventilation losses and is defined as:

$$Q_z=Q_T+Q_V \tag{2}$$

where Q_T represents the transmission losses, and Q_V represents the ventilation losses. Transmission losses occur during the transfer of heat from the zone to the external environment. The boundary surfaces for heat transfer are the walls, ceiling, floor, windows, and doors. It is necessary to calculate the transmission losses through all these surfaces, which are defined as:

$$Q_T = \left(\sum_{i=1}^{n} H_{T,i}\right) \cdot \Delta t \tag{3}$$

where $H_{T,i}$ is the individual transmission loss coefficient from the heated space to the external environment, and Δt represents the temperature difference between the internal temperature and the external environment.

The individual transmission loss coefficients from the heated space to the external environment [W/K] are calculated as:

$$H_{T,i} = A_i \cdot U_i \cdot e_i \tag{4}$$

where A_i is the surface area of the building element (wall, window, door, ceiling, etc), U_i is the heat transfer coefficient of that building element, and e_i is the exposure correction factor, which is set to 1 to be consistent with the guideline of EN 12831 standard [11].

Ventilation heating losses are defined as:

$$Q_V=H_{V,i} \cdot (t_u - t_s) \tag{5}$$

where $H_{V,i}$ is the coefficient of ventilation heat losses, t_u is the internal temperature, and t_s is the external temperature.

C. *Model of Internal Heat* Gains

Internal heat gains originate from:

- People
- Lighting
- Devices

In this paper, the impact of lighting and devices will be neglected, while the heat gain from people will still be considered. To synthesize the model of internal heat gains from people, it is necessary to know the amount of heat energy that people release while staying in the room.

It should be noted that this value varies depending on the type of activity that people engage in within the room. The data are taken from the ASHRAE handbook [12,13] and are presented in Table I.

TABLE I. Estimated heat energy emitted by people

Activity	***Feel [W]***	***Latent [W]***	***Total [W]***
Siting	70	30	100
Siting (easy labor)	75	45	120
Standing	75	70	145
Light labor	90	160	250
Heavy labor	185	285	470

Based on the estimated heat energy emitted by people in Table 1, the following equation represents heat energy emitted by a group of people based on their activities, and it is defined as follows [14, 15]:

$$\dot{Q}_p=n_s\cdot 70+n_{st}\cdot 75+n_l\cdot 90+n_t\cdot 185 \tag{6}$$

where n_s is the number of people sitting, n_{st} is the number of people standing, n_l is the number of people performing light labor, and n_t is the number of people performing heavy work.

D. Heating element model

The heat balance equation of the heating element is defined as:

$$\dot{Q}_g=\dot{Q}_a+\dot{Q}_r \tag{7}$$

where Q_g represents the heat energy supplied to the heating element (radiator), Q_a represents the accumulated heat energy, and Q_r represents the heat energy emitted to the surroundings [16].

The detailed mathematical model for the heat balance equation of the heating element is defined as follows:

$$\dot{m}_w\cdot c_w\cdot(T_{in}-T_{out})=K_1\cdot\frac{dT}{dt}+\dot{Q}_n\cdot\left[\frac{\Delta t}{\Delta t_n}\right]^n \tag{8}$$

$$K_1=(m_v\cdot c_w+m_m\cdot c_m) \tag{9}$$

where m_v is the mass flow rate of hot water to the radiator, c_w is the specific heat capacity of water, m_w is the mass of water in the radiator, m_m is the mass of the radiator's metal cover, c_m is the specific heat capacity of the radiator's metal, Q_n the nominal power of the radiator for the given type, measured according to the EN 442 standard, Δt is the logarithmic temperature difference, Δt_n is the logarithmic temperature difference calculated for the selected temperature regime (90/70/20 ˚C), and n is the characteristic exponent for the given type of radiator.

TABLE II. PARAMETERS OF THE THERMAL SYSTEM MODEL

Parameter	*Symbol*	*Value*	*Unit*
Wall surface	A_w	81.64	m^2
Floor/Ceiling surface	A_f / A_c	40	
Door surface	A_d	2.6	
Window surface	A_{wd}	2.8	
Wall heat transfer coefficient	U_w	0.29	[W/m$_2$K]
Floor heat transfer coefficient	U_f	0.4	
Ceiling heat transfer coefficient	U_c	0.3	
Door heat transfer coefficient	U_d	1.3	
Window heat transfer coefficient	U_{wd}	1.2	
Water mass (radiator)	m_v	10.56	kg
Metal mass (radiator)	m_m	53.44	
Radiator inlet temperature	T_{in}	90	[˚C]
Heat capacity water	c_w	4.2	[kJ/kgK]
Heat capacity c metal	c_m	0.490	
Characteristic exponent (radiator)	n	1.3358	-

IV. EXPERIMENTAL APPROACH

A. Experimental configuration

In forming the HIL system, specific hardware must be used to manage and perform real-time simulations. For the control system in this study, the Schneider Electric (SE) AS-B-24 [17] controller will be used with Schneider Electric's EcoStruxure programming and management environment, which provides an efficient platform for designing and implementing control logic. This platform provides various control logics, including the PID control algorithm. The mathematical representation of the discrete-time PID controller is given by:

$$\Delta u(t)=G\cdot\left[e(t)-e(t-h)+\frac{h}{T_i}\cdot e(t)-T_d\cdot\frac{y(t)-2\cdot y(t-h)+y(t-2h)}{h}\right] \tag{10}$$

where G is the controller gain, e(t) is the control error, h is the control interval (time between successive updates), T_i is the integral time constant, T_d is the derivative time constant, and y(t) is the measured process variable.

The T_d parameter was set to zero, reducing the controller to a PI (proportional-integral) structure. The controller gain G is set to 2.3 and Ti to 6.9, tuned experimentally using a step-response method [18]. The simulation of the thermal zone will be carried out on the National Instruments (NI) sbRIO-9636

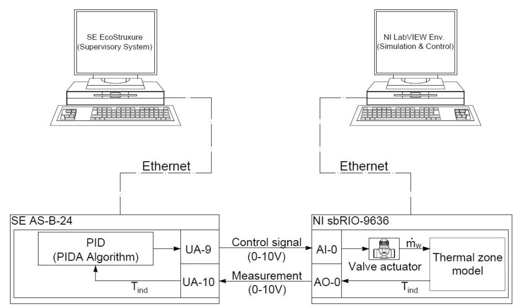

Fig. 2. Experimental configuration of devices

[19] controller. The National Instruments sbRIO-9636 controller is equipped with a Real-Time processor and an FPGA on the same chip, which is essential for its real-time operation. This architecture enables precise timing and deterministic execution, making it suitable for highly responsive applications. In this study, the control loop operates at a frequency of 1 kHz to ensure accurate real-time performance. It should be noted that a time step of 10 seconds is selected due to the relatively slow dynamics of temperature variation, which allows for sufficient resolution without unnecessary computational overhead.

It should be mentioned that the room temperature is considered uniform, following the lumped capacitance model. Instead of using a physical sensor, a mathematical model calculates the temperature within the NI controller. The simulated temperature is then used as feedback, effectively replicating the function of a real-world temperature sensor.

The main governing equation used in the LabVIEW to predict the variation of the heated space temperature with time was derived from Equation (1) and is shown by the following equation:

$$\rho_{air}\cdot c_{air}\cdot V_{air}\cdot\frac{dT_{in}}{dt}=\dot{Q}_p+\dot{Q}_w-\dot{Q}_z-\dot{Q}_i \tag{11}$$

where ρ_{air} is the density of the air, c_{air} is the specific heat capacity of air, V_{air} is the air volume in the zone, and T_{in} is the indoor temperature of the zone.

The analog output from the NI controller transmits information about the current temperature in the zone. This signal is sent to the SE controller, which calculates the error based on the reference value (20˚C) using the PIDA control algorithm. The SE controller then generates control signals, which are processed in the NI controller and used to regulate the valve opening of the radiator heating system.

It should be noted that both controllers are connected to PCs via an Ethernet connection, where the current values of the simulation parameters and control actions are displayed.

B. Experimental results

Two simulations were conducted to validate the functionality of the HIL system and verify the proper operation of the simulation model and control system. Figures 3 and 4 illustrate the simulated temperature changes within the zone, while the transient response specifications are summarized in Table II. The outside temperature of both Simulation I and Simulation II was set to 5 °C. The main distinction between the simulations is the width of the insulated wool material used in walls. In Simulation I, the width of insulated wool material is 100mm, whereas, in the second simulation, it was reduced to 50mm. A tolerance bound of ±5% of the set point value was imposed, consistent with the guideline that the maximal allowable temperature variation for comfort is 1.1 °C [11], which equates to approximately ±5%.

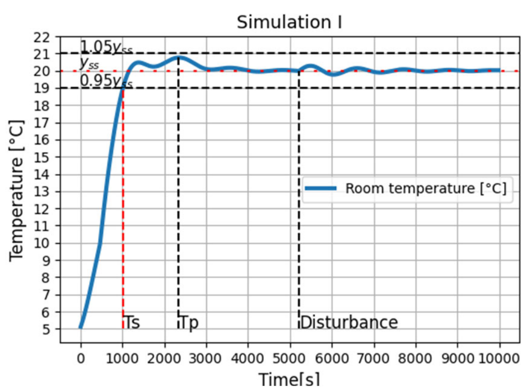

Fig. 3. Simulation I results

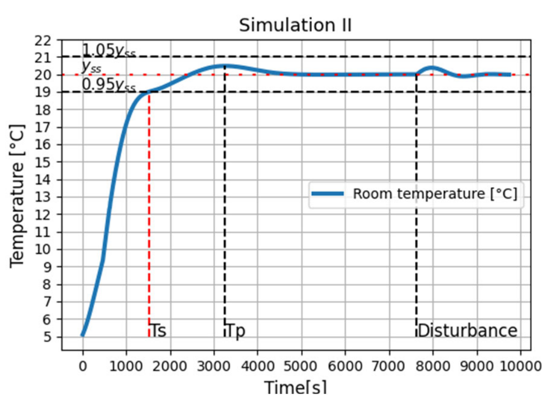

Fig. 4. Simulation II results

The primary factor contributing to the difference in transient response specifications between Simulation I and Simulation II is the insulation thickness of the walls. This change directly impacts the thermal properties of the walls, which affects heat retention, thermal resistance, and thermal inertia of the model.

TABLE III. TRANSIENT RESPONSE SPECIFICATIONS

Specifications	***Simulation I***	***Simulation II***	***Units***
Set point (y_{ss})	20	20	°C
Rise time (t_r)	920	1120	s
Settling time (t_s)	1080	1520	s
Peak time (t_p)	2350	3250	s
Overshoot	3.79	2.4	%
Steady-State error (e_{ss})	0.106	0.08	%
Temp at t_p (max temp)	20.758	20.48	°C
Disturbance	5223	7637	s

V. DISCUSSION

The simulation of the thermal zone was performed as expected, successfully following the task of reaching the target values. The PID control law successfully compensates for the additional disturbances and manages to maintain the temperature within the desired range.

Results show that thicker insulation provides greater thermal resistance, reducing heat transfer through the walls, which leads to less heat loss to the environment and a more stable internal temperature. Thicker insulation minimizes the effect of external temperature changes, which leads to shorter settling time (faster stabilization) and lower rise time. On the other side, thinner insulation causes less thermal resistance, allowing more heat to escape through the thermal envelope, and consequently, the system needs more time and energy to maintain the desired temperature. Ultimately, this leads to longer rise and settling times, as the control system must work harder to compensate for heat losses.

The system with thicker insulation exhibits a higher overshoot (3.79%) compared to the thinner insulation (2.4%). The reason is that thicker insulation retains more heat in the thermal zone, causing a temporary overshoot before the system stabilizes. The small difference in overshoot between the two cases shows that the mathematical model accurately captures the thermal dynamics of the system. Additionally, thicker insulation results in shorter rise and settling times, enhancing the system's thermal response. Thinner insulation prolongs these times due to higher heat exchange with the external environment.

VI. CONCLUSION

In this paper, a mathematical model was developed and implemented on a hardware platform, and a thermal zone was simulated. Two simulations were performed: Simulation I with thicker and Simulation II with thinner wall insulation. Disturbances were introduced in both simulations. This study shows promising results achieved in residential and commercial building heating and cooling processes based on experimental results. Based on the conclusions and results, further research is necessary to establish a more precise and detailed thermal zone and HIL environment model.

ACKNOWLEDGMENT

This research has been supported by the research grants of the Serbian Ministry of Science, Technological Development and Innovations, grant No. 451-03-136/2025-03/ 200066.

REFERENCES

[1] A. FSK Agyemang, R. Memon, and S. Fox, "Mapping urban living standards and economic activity in developing countries with energy data," PLOS ONE, vol. 18, no. 9, p. e0291824, September 2023.

[2] N. Irtija, F. Sangoleye, and E. E. Tsiropoulou, "Contract-Theoretic Demand Response Management in Smart Grid Systems," IEEE Access, vol. 8, pp. 184976-184987, October 2020.

[3] S. Attia, "Spatial and Behavioral Thermal Adaptation in Net Zero Energy Buildings: An Exploratory Investigation," Sustainability, vol. 12, no. 19, p. 7961, September 2020.

[4] G. Li, Z. Yang, Y. Fu, Z. O'Neill, L. Ren, O. Pradhan, and J. Wen, "A hardware-in-the-loop (HIL) testbed for cyber-physical energy systems in smart commercial buildings," Sci. Technol. Built Environ., vol. 30, pp. 1–18, 2024.

[5] I. Inayat, R. u. Amin, and M. M. Ali, "Hardware-in-the-loop flight motion simulation of flexible variable sweep aircraft," Aircraft Eng. Aerospace Technol., vol. 90, no. 9, pp. 1428–1437, 2018.

[6] L. Cabeza, D. Veréz, and M. Teixidó, "Hardware-in-the-loop techniques for complex systems analysis: bibliometric analysis of available literature," Appl. Sci., vol. 13, no. 14, p. 8108, July 2023

[7] G. F. Schneider, J. Oppermann, A. Constantin, R. Streblow, and D. Müller, "Hardware-in-the-Loop-Simulation of a Building Energy and Control System to Investigate Circulating Pump Control Using Modelica," Linköping Electron. Conf. Proc., vol. 118, p. 225-233, September 2015.

[8] Z. Chen, J. Wen, S. T. Bushby, L. J. Lo, Z. O'Neill, W. V. Payne, A. Pertzborn, C. Calfa, Y. Fu, G. Grajewski, Y. Li, and Z. Yang, "Development of a Hardware-in-the-loop Testbed for Laboratory Performance Verification of Flexible Building Equipment in Typical Commercial Buildings," arXiv preprint, arXiv:2301.13412, January 2023.

[9] F. Mihalić, M. Truntić, and A. Hren, "Hardware-in-the-Loop Simulations: A Historical Overview of Engineering Challenges," Electronics, vol. 11, no. 15, p. 2462, August 2022.

[10] S. Attia, "Spatial and Behavioral Thermal Adaptation in Net Zero Energy Buildings: An Exploratory Investigation," Sustainability, vol. 12, no. 19, p. 7961, September 2020.

[11] European Committee for Standardization, SRPS EN 12831-1:2017: Energy performance of buildings – Method for calculation of the design heat load – Part 1: Space heating load, Module M3-3, 2017.

[12] ASHRAE, Standard 55: Thermal Environmental Conditions for Human Occupancy, American Society of Heating, Refrigerating and Air-Conditioning Engineers, Atlanta, GA, 2020.

[13] J. F. Kreider, P. S. Curtiss, and A. Rabl, *Heating and Cooling of Buildings: Design for Efficiency*, 2nd ed., CRC Press, 2009, pp. 321.

[14] O. Alhaj Hasan, "Optimization of building energy consumption using simplified models and new control methods," Ph.D. dissertation, 2014.

[15] T. Ogedengbe and T. Erinle, "Computer-Aided Load Estimation of Air-conditioning Systems for Non-residential and Residential Buildings," 18, pp. 161-172, 2015.

[16] L. Chen and B. R. Sørensen, "Modelling Multilayer Hydronic Radiators," E3S Web Conf., vol. 172, p. 12007, 2020.

[17] Schneider Electric, "SpaceLogic automation server, AS-B-24," Revision, September 2022. [Online]. Available: https://www.se.com/uk/en/product/SXWASB24PX10001/spacelogic-automation-server-asb24-24-i-o-points-bacnet-ms-tp-modbus-scalable/. [Accessed: Jan. 23, 2025].

[18] G. Kvaščev and M. Mataušek, "Application of PLC controllers in the implementation of automatic setting of PI regulators from the step response," Master's thesis, University of Belgrade, Faculty of Electrical Engineering, September 2000.

[19] National Instruments, "OEM OPERATING INSTRUCTIONS AND SPECIFICATIONS NI sbRIO9636," Revision, March 2013. [Online]. Available:https://www.ni.com/en-rs/support/model.sbrio-9636.html?srsltid=AfmBOoqEDI6jqDpnjzrW7Cqz_LE2-RwwaFgkxeJWVbwlU_c84a-7Mkoj. [Accessed: Jan. 23, 2025].